

Redshift dependence of clustering in numerical simulations

VOLKER MÜLLER

Astrophysical Institute Potsdam

High resolution N -body simulations for variants of the CDM model are used to derive the redshift dependence of galaxy formation and of galaxy correlation functions. The reconstructed power spectra and clustering properties provide a sensible test for the underlying power spectra. We compare our simulations with new results of the analysis of recent redshift surveys. The results are used to discuss the model of primordially broken scale invariant perturbations (BSI).

1. INTRODUCTION

Biased structure formation in a flat universe dominated by cold dark matter (CDM) has difficulties in describing the formation of large-scale structure in the universe, it delivers too small large-scale power for getting the microwave background anisotropies, large scale velocity fields, and cluster-cluster correlations. On the other hand, *unbiased* (COBE normalised) CDM seems to have too much small scale power for describing the galaxy clustering and small scale velocity fields. This was our motivation for discussing double inflationary models which provide perturbation spectra with enhanced power at large scales (Broken Scale Invariant perturbations – BSI, Gottlöber et al. 1991). The redshift dependence of gravitational clustering of the new theory in comparison with COBE-normalised standard CDM enlightens its pros and cons.

To this aim we performed a series of high-resolution PM simulations, with a model for the thermodynamic evolution of baryons (cp. part III and Kates et al. 1995 for details and chosen parameters). The superposition of simulation boxes with different scales allows the study of structure formation over a wide range of cosmic scales. The 'thermodynamic' properties are used as an additional indicator for dissipative processes in the high density regions, and therefore, for the time dependence of the condensation of cosmic structures. It is interesting that the filamentary structure becomes visible in the distribution of both 'cold' particles and warm ($\approx 10^6$ K) gas.

We use density peaks in the *cold* matter for identifying 'galaxy' halos with a reasonable mass spectrum, and we compare their clustering properties and power spectra with data from large galaxy catalogues. Next we will discuss the redshift evolution of the two-point correlation function using peak-selected mass particles. Finally, we compare our results with data from observations, and we draw some conclusion.

II. DOUBLE INFLATION SCENARIO

Double inflation is an old idea which requires for example two basic scalar fields in the fundamental theory (Starobinsky 1985). We derived in detail the conditions for the occurrence of two inflationary stages separated by an intermediate dust-like phase (Gottlöber et al. 1991). This is necessary for getting a sharp break in the primordial power spectrum. Further, we select the parameters so that this break lies at the comoving scale corresponding approximately to the turn around radius of galaxy clusters. Then we have a typical scale which separates 'large' and 'small' cosmic structures. A description of the power of primordial potential perturbations $P_{\Phi}(k)$ is given by the approximation (it does not describe the typical oscillations generated during the intermediate power law stage),

$$k^3 P_{\Phi}(k) = \begin{cases} 4.2 \times 10^{-6} [\log(k_s/k)]^{0.6} + 4.7 \times 10^{-6} & \text{for } k < k_s \\ 9.4 \times 10^{-8} \log(k_f/k) & \text{for } k > k_s \end{cases}$$

Here, $k_s = (2\pi/24)h^{-1}\text{Mpc}$, $k_f = e^{56}h^{-1}\text{Mpc}$. We considered a cosmological model with the dimensionless density parameter $\Omega = 1$, dominated by cold dark matter (CDM), and we use a dimensionless Hubble constant $h = 0.5$. The initial power spectrum rescaled by linear theory to redshift $z = 0$ is shown by the dash-dotted line in Fig. 1. For comparison we show the CDM curve as dotted line.

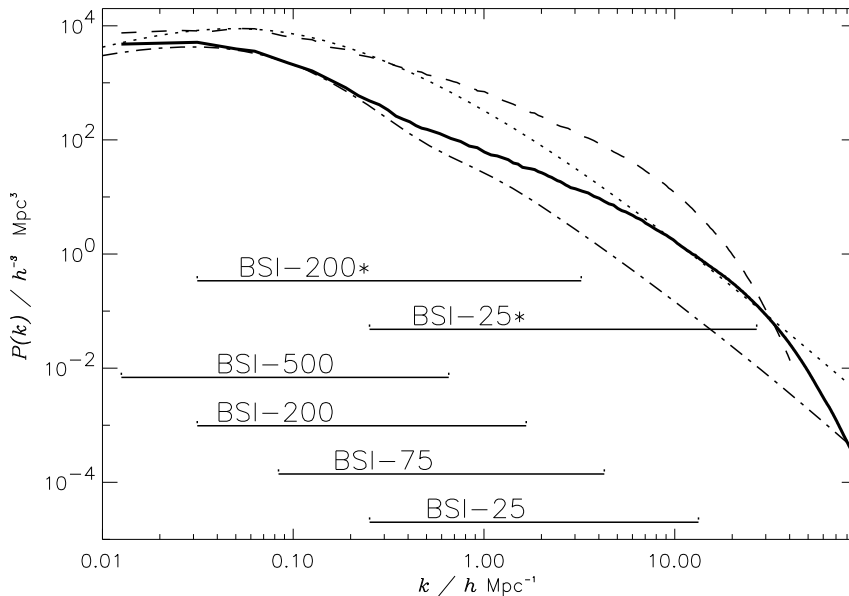


FIGURE 1. Linear and non-linear BSI (dash-dotted and solid lines) and CDM (dotted and dashed lines) power spectra of density fluctuations at $z = 0$.

An alternative model which uses a feature in the scalar field potential was discussed by Semig and Müller (1995). It describes the transition of a self-interacting to a massive scalar field, in consequence it leads to a valley-like shape of the primordial potential spectrum. All the power spectra used in the simulations are normalised at large scales by the measured anisotropy of the microwave background radiation (cp. Gottlöber and Mückel 1993).

III. N-BODY SIMULATIONS AND GALAXY IDENTIFICATION

At present no theoretical description or simulation scheme exhausts all the various effects of structure formation in the universe. For testing our envisaged model we have to study both the large scale structure formation, i.e. the formation of clusters and superclusters of galaxies, and the formation of the different types of galaxies as the basic building blocks of all large cosmic structures.

To this end, we perform a set of simulations with box sizes ranging from 25 h^{-1} Mpc for having enough resolution at galactic scales, to 75 h^{-1} Mpc and 200 h^{-1} Mpc for studying galaxy clustering, and to 500 h^{-1} Mpc for the super-large scale structure (in Fig. 1 the covered wavenumber range is schematically indicated). We use the PM code of Kates, Kotok, & Klypin (1991), taking for BSI in the highest resolution 512^3 cells and 256^3 particles (simulation names with asterisk in Fig. 1) and a set of simulations with half the resolution for comparing BSI and CDM (Kates et al. 1995). The solid line in Fig. 1 shows the combined non-linear spectrum of the dark matter after evolving from redshift $z = 25$ to the present. The higher non-linear power of the corresponding CDM-simulations is shown by the dashed line.

During the simulation the code is looking for shocks between triplets of originally neighboring particles, which are given by the changes of the sign of the volume spanned by these particles. At shocks we attribute to particles with velocity \vec{v} a 'temperature', $kT \approx \mu_M m_H (\vec{v} - \vec{U})^2/3$, where \vec{U} is the local velocity determined by interpolation of the velocity field onto a twice coarser grid. Subsequently, we suppose each particle has properties both of dark and baryonic matter (we use a cosmic abundance of 10% baryons). The baryonic gas is allowed to cool and, during gravitational collapse, it also gets adiabatically heated. Further we take into account feedback mechanisms which result from star formation and subsequent SN-explosions. It reheats a certain part of the cold gas (85%, this percentage was taken over from the older simulations). This recipe leads to a reasonable account of the condensation of baryonic matter in galactic halos and its clustering. Since we do not alter the dynamics during and after shocks, dark and baryonic matter remains in the same pattern.

Due to the nonlinear gravitational instability a large part of 'baryons' (up to 88%) gets 'cold' and transforms to stars and star systems. Galaxies are identified with density maxima in the distribution of cold particles which lie over a certain threshold (2 to 3 times the grid variance), but 'galaxy halos' are assembled by all particles within a search radius of 0.5 times the mean interparticle separation. The resulting mass distributions can be fitted by a Schechter function

$$dn/d \log M = (n_* M/M_*)^{-p} \exp(-M/M_*),$$

For BSI-25* we get $M_* = 10^{12} M_\odot$, $n_* = 2.6 \times 10^{-2} h^3 Mpc^{-3}$ and $p = 0.8$. This is a quite reasonable density of M_* galaxies (corresponding possibly to L_* galaxies). The derived galaxy catalogues are used to compare the consequences of the model with characteristics of the large scale matter distribution in the universe.

III. POWER SPECTRA AND CORRELATION FUNCTION

The described galaxy identification scheme leads to a physical biasing model. We used counts in cell variances as a robust measure of the large scale bias (integral bias due to Cen and Ostriker, 1992) as a characteristic of the derived galaxy catalogues. We get in the BSI model 'naturally biased' galaxies with a bias parameter $b \approx 1.5$ which does not strongly depend on the scales. On the other hand,

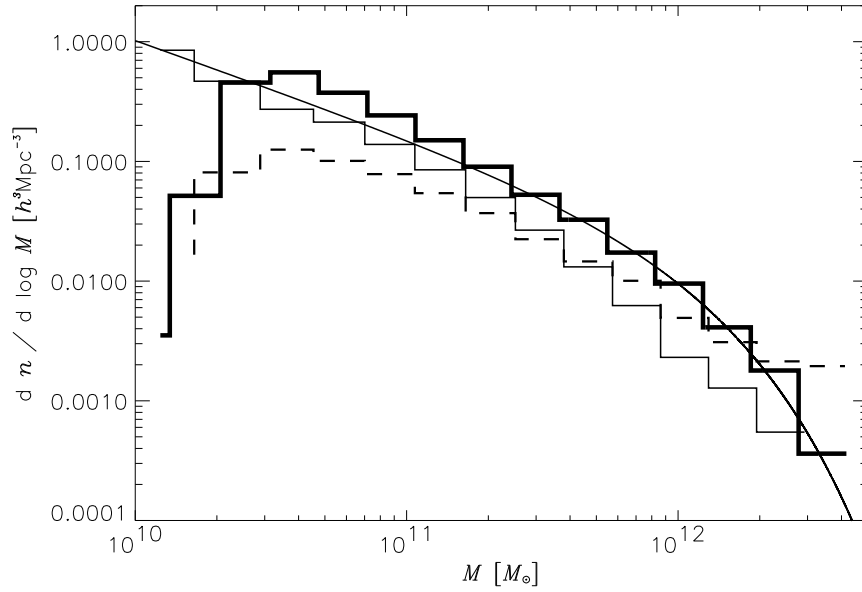


FIGURE 2. The galaxy mass function of BSI-25 (solid histogram), BSI-25*(thick solid histogram), and CDM-25 (dashed histogram). The parameters of the fitting Schechter function are given in the text.

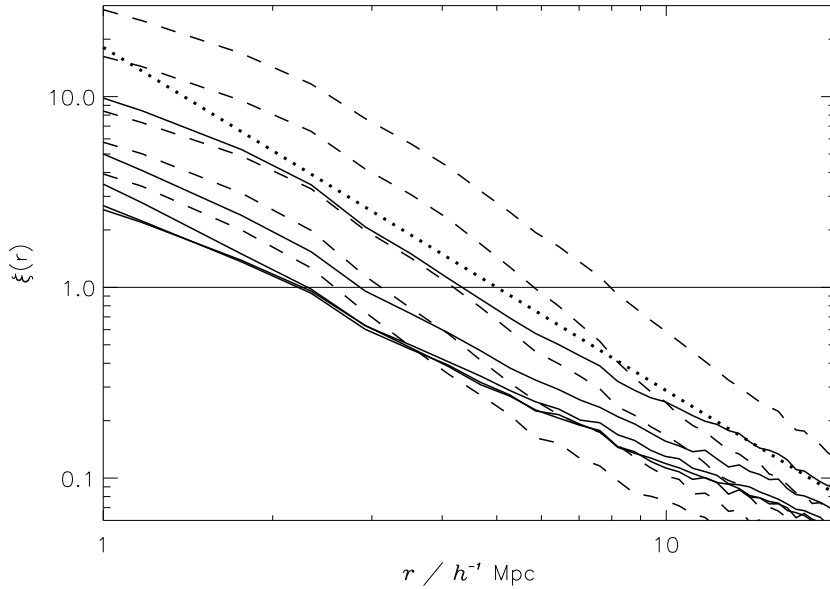


FIGURE 3. Redshift evolution of the correlation function in BSI-75 and CDM-75, where on DM particle corresponds to $10^{11} M_{\odot}$.

'clusters of galaxies', identified in the larger simulation boxes, have $b \approx 3$ (Kates et al. 1995). The question whether these values of the bias parameter are realistic has been discussed using the redshift dependence of the two-point correlation function.

Here, we used for computational convenience particles in cells with overdensity of about 30 as tracers of the galaxy distribution in BSI. This threshold is a compromise between the overdensity expected for virialised halos and the finite resolution in the PM-simulations. For the CDM simulations, we suppose no biasing at all. In Fig. 3 we show the correlation functions at redshifts $z = 2, 1.5, 1, 0.5, 0$ (increasing from below) for BSI-75 (solid lines), and CDM-75 (dashed line). The dotted line is about the observed curve

$$\xi = (r/r_0)^{-1.8}$$

with $r_0 = 5 h^{-1}\text{Mpc}$. As it is well known, the CDM curves are rising strongly even in comoving coordinates during the redshift interval studied. For the chosen normalisation, the 'correct' amplitude and slope is reached about at redshift $z \approx 1$. In the contrary, for the BSI model we find between $z = 2$ and $z = 1$ a stable clustering in *comoving coordinates*, and later an increase of the slope and amplitude about up to the observed values. In Amendola et al. (1995) we used these peak selected 'galaxy catalogues' for a comparison with the APM angular correlation function, which is reasonably reproduced in the BSI model. Now we consider the comparison with galaxy redshift catalogues using galaxies selected from density maxima in the cold gas as described above (cp. Fig. 2).

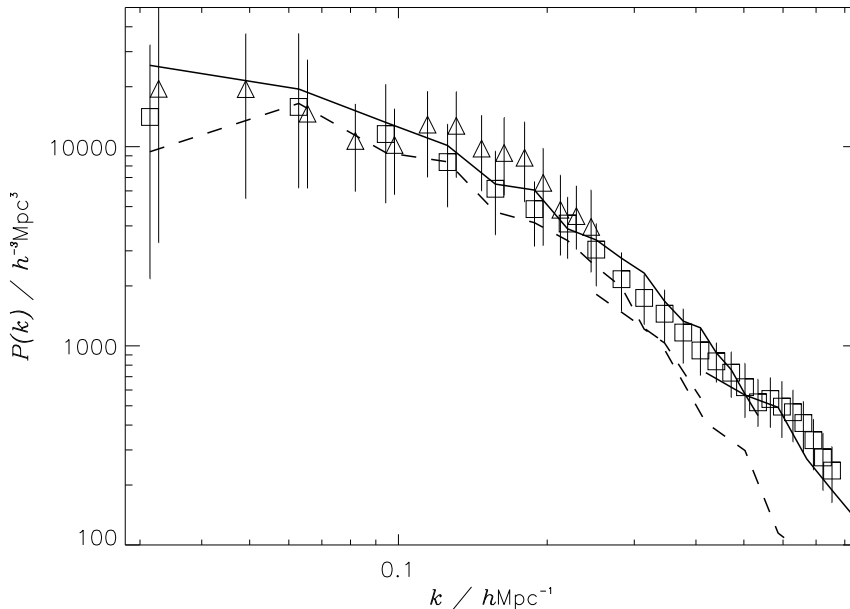


FIGURE 4. Comparison with BSI (solid line) and CDM (dashed line) galaxy power spectra from CfAII (squares) and IRAS (triangles).

First we describe the comparison of simulated power spectra with the power spectrum reconstructed from the CfA galaxy catalogue (Vogeley et al. 1992). We impose redshift corrections by placing an arbitrary observer far outside the simulation box. The resulting power spectrum of BSI and CDM galaxies, identified in simulations with a box length of $200 h^{-1}\text{Mpc}$ is shown in Fig. 4, where we select 'galaxies' with more than 10 particles for BSI and over 30 particles for CDM (the higher threshold is due to the more advanced clustering in the CDM model). The

CDM model is strongly influenced by the redshift corrections which enhance the power near the maximum, and they suppress the power at higher k values (another cause for suppression of the power at high wave numbers is the subtraction of shot noise). Both spectra can fit the CfA power spectrum, in particular the BSI model leads to a very good fit of the data. The galaxies used in this simulation are biased with respect to the sea of all dark matter particles by an (approximately linear) bias factor of about 2, contrary to the CDM model which has $b \approx 1$.

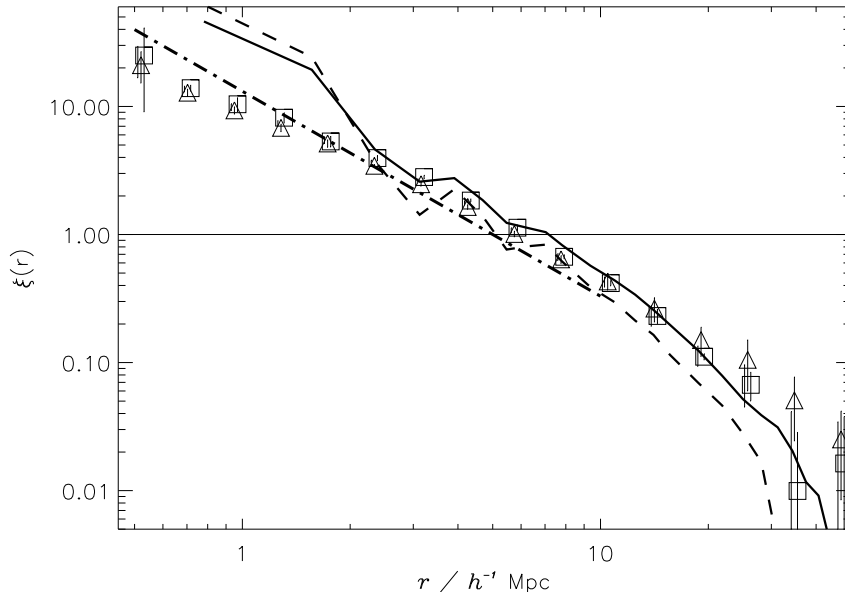


FIGURE 5. Comparison with the two-point correlation in BSI (solid line) and CDM (dashed line) with results from the Las Campanas survey (triangles: number weighted, squares: luminosity weighted).

The galaxy correlation function shown in Fig. 5 supplements the study of the power spectrum. While in principle it has the same information content, the accuracy of its estimation is much higher in the region of nonlinear clustering. Here we compare 'galaxies' composed of a minimum number of 5 and 10 particles in the BSI-75 and CDM-75 simulations, respectively. The data of the Las Campanas Deep Redshift Survey are taken from Tucker et al. (1995). Again, due to redshift corrections both curves are able to reproduce the observed galaxy clustering over a wide range of scales (in the contrary, the real space correlation function of CDM galaxies is much steeper than that of BSI galaxies, cp. Fig. 3). The lower clustering level of the data at lengths below $2 h^{-1}\text{Mpc}$ is probably due to selection effects. A small difference becomes visible in the length range $(20 - 30) h^{-1}\text{Mpc}$, where the higher clustering of the LCDRS galaxies may indicate an enhanced power, it is slightly better reproduced by the BSI model. The dash-dotted line shows the power law $\xi = (r/r_0)^{-1.6}$ with $r_0 = 5 h^{-1}\text{Mpc}$.

IV. CONCLUSIONS

Strong differences between the properties of galaxies in the two models become visible in the small scale velocity dispersion. Its one dimensional (line of sight)

projection value lies at about 250 km/s in the BSI model and at about 600 km/s in the CDM model. This velocity dispersion can be estimated from the anisotropy of the two-point correlation function of galaxy redshift catalogues with respect to the line of sight and orthogonal to it. Further strong differences come from the observed mass distribution of galaxy clusters and the cluster-cluster correlation function (Müller 1994). In the BSI model, the latter remains positive on scales up to at least $60 h^{-1}\text{Mpc}$. On the other hand, the high degree of clustering in the CDM model is connected with large velocity fields on small scales, which weakens the clustering signal if observed in redshift space. Therefore, the two-point correlation function and power spectra have difficulties in distinguishing between the two models. More elaborate tests take into account the properties of galaxy clusters and large scale velocity fields. Complementary to the evolution of the correlation function, both models can be clearly distinguished in the redshift evolution of the characteristic scales of pancakes and filaments identified by more refined statistical methods (Doroshkevich et al. 1995).

REFERENCES

- Gottlöber, S., Müller, V., Starobinsky, A.A., 1991, *Phys.Rev.*, D43, 2510.
 Kates, R., Müller, V., Gottlöber, S., Mückel, J.P., Retzlaff, J., 1995, *MNRAS* in press, astro-ph/9507036.
 Starobinsky, A.A., 1985, *Sov.Astron.Lett.*, 9, 302.
 Semig, L., Müller, V., 1994, *A&A* in press, astro-ph/9508020.
 Gottlöber, S., Mückel, 1993, *A&A* 272, 1.
 Kates, R., Kotok E., Klypin, A. 1991, *A&A* 243, 295.
 Cen, R., Ostriker, J.P., 1992, *ApJ* **399**, L113.
 Amendola, L., Gottlöber, S., Mückel, J.P., Müller, V., 1995, *ApJ* in press, astro-ph/9408104.
 Vogeley, M., Park, C., Geller, M., Huchra, J.P., 1992, *Astroph. J.* **391**, L5.
 Tucker, D.L., Oemler, A.A., Kirshner, R.P., Lin, H., Shectman, S.A., Landy, S.D., Schechter, P.L., 1995, Proc. XXX Moriond-Meeting "Clustering in the Universe".
 Müller, V., 1994, in: 'Cosmological Aspects of X-Ray Clusters of Galaxies', ed. W.C. Seitter, Kluwer, NATO ASI Series, 441.
 Doroshkevich, A.G., Fong, R., Gottlöber, S., Mückel, J.P., Müller, V., 1995, *MNRAS* subm, astro-ph/9405088.